Biology Faculty Scholarship   College of the Sciences

1-31-2023

Differential Strain-Dependent Ovarian and Metabolic Responses in a Mouse Model of PCOS

April K. Binder

Danielle L. Peecher

Amanda J. Qvigstad

Silvia D. Gutierrez

Jennifer Magaña

See next page for additional authors

Authors

April K. Binder, Danielle L. Peecher, Amanda J. Qvigstad, Silvia D. Gutierrez, Jennifer Magaña, David B. Banks, and Kenneth S. Korach

1 **Differential Strain-Dependent Ovarian and Metabolic Responses in a Mouse Model of**

2 **PCOS**

3 April K. Binder[1,2,3], Danielle L. Peecher[1,2], Amanda J. Qvigstad[1,2], Silvia D. Gutierrez[1,2], Jennifer

4 Magaña[1,2], David B. Banks[3,4] & Kenneth S. Korach[3]

5 [1]Central Washington University, Biological Sciences, Ellensburg, WA

6 [2]Center for Reproductive Biology, Washington State University, Pullman, WA

7 [3]Reproductive & Developmental Biology Laboratory, NIEHS, NIH, Research Triangle Park, NC

8 [4]University of Chicago Hospitals and School of Medicine, Chicago, IL

9 Running Title: Mouse Strain Dependent PCOS Phenotype

10 Keywords: PCOS, DHT, mouse, ovary, adipose

11

12 Correspondence:

13 April K Binder

14 Central Washington University

15 Department of Biological Sciences

16 400 E University Way MS7537

17 Ellensburg, WA 98926

18 TEL (509)963-2803

19 E-Mail: april.binder@cwu.edu

20 ORCHID: 0000-0002-4095-4947

21

26

1 **Abstract**

2 Several mouse models have been developed to study polycystic ovarian syndrome (PCOS), a

3 leading cause of infertility in women. Treatment of mice with dihydrotestosterone (DHT) for 90-

4 days causes ovarian and metabolic phenotypes similar to women with PCOS. We used this 90-

5 day DHT treatment paradigm to investigate the variable incidence and heterogeneity in two

6 inbred mouse strains, NOD/ShiLtJ and 129S1/SvlmJ. NOD mice naturally develop type 1

7 diabetes, and recent meta-analysis found increased androgen excess and PCOS in women with

8 type 1 diabetes. 129S1 mice are commonly used in genetic manipulations. Both NOD and

9 129S1 DHT treated mice had early vaginal opening, increased anogenital distance and altered

10 estrus cycles compared to control animals. Additionally, both NOD and 129S1 mice had

11 reduced numbers of corpora lutea after DHT exposure, while NOD mice had decreased

12 numbers of preantral follicles and 129S1 mice had reduced numbers of small antral follicles.

13 NOD mice had increased body weight, decreased white adipocyte size, and improved glucose

14 sensitivity in response to DHT, while 129S1 mice had increased body weight and white

15 adipocyte size. NOD mice had increased expression of *Adiponectin, Cidea, Srebp1a and*

16 *Srebp1b* and 129S1 mice had decreased *Pparg* in the white adipose tissues, while both NOD

17 and 129S1 mice had increased expression of *Glut4* and *Prdm16* suggesting DHT may

18 differentially affect glucose transport, thermogenesis, and lipid storage in white adipose tissue.

19 DHT causes different ovarian and metabolic responses in NOD and 129S1 mice suggesting that

20 strain differences may allow further elucidation of genetic contributions to PCOS.

21

22 **Introduction**

23 Polycystic ovarian syndrome (PCOS) is a leading cause of infertility in females of reproductive

24 age, affecting approximately 5-15% of women depending on the study and criteria used for

25 diagnosis (1–5). Women with PCOS present with heterogeneous symptoms, making diagnosis

26 and clinical studies challenging. Current clinical diagnosis uses the Rotterdam criteria, where

1 patients must exhibit two of the following three symptoms: clinical or biochemical

2 hyperandrogenism, oligo- or amenorrhea, and the presence of polycystic ovaries by ultrasound

3 (4,6). In addition to these symptoms, women with PCOS often have metabolic disorders,

4 including obesity, insulin resistance and type 2 diabetes, hyperinsulinemia, dyslipidemia, and

5 increased risk for cardiovascular disease (4,7–9).

6 Several animal models have been developed in chimpanzees, sheep, and rodents to study

7 various aspects of PCOS. Many models are established by introducing excess androgens to

8 drive PCOS phenotypes (10–17). In mice, androgen treatments using 5α-dihydrotestosterone

9 (DHT) and dehydroepiandrosterone (DHEA) have been administered both pre- and postnatally

10 to produce a model replicating the reproductive and metabolic phenotypes commonly observed

11 in women with PCOS (10,11). Implantation of 90-day slow-release DHT pellets into prepubertal

12 mice has been shown to cause PCOS phenotypes including ovarian and metabolic dysfunction

13 (18,19), although this model has been used almost exclusively in the inbred strain of C57BL/6

14 (B6) mice.

15 PCOS is reported to have a genetic component in women (4,15,20). Herein, we sought to

16 examine the role of genetic background in PCOS by using two inbred mouse strains:

17 NOD/ShiLtJ and 129S1/SvlmJ both founder strains in the collaborative cross mice, a

18 recombinant inbred mouse resource developed for complex trait analysis (21–23). Non-obese

19 diabetic or NOD/ShitLtJ (NOD) mice spontaneously develop type I diabetes (T1D) around 12-14

20 weeks (24), with 60-80% of females affected while only 20-30% of males are affected at this

21 age (25). This occurs due to an autoimmune attack on pancreatic endocrine tissue leading to

22 insulitis and decreased levels of insulin (26). A meta-analysis found an increased prevalence of

23 PCOS and androgen excess in women with type I diabetes (T1D) compared to women without

24 diabetes (27). The use of NOD mice may provide insight into the genetic background influences

25 on the PCOS phenotype and how T1D may influence a predisposition and susceptibility for

26 developing PCOS.

129S1/SvlmJ (129S1) mice are an embryonic stem cell source for genetic manipulations and studies of diet-induced weight gain in 129S strains of mice have varied results. One study reported high-fat diet (HFD) induced a larger risk for inflammatory stress in the kidneys and liver in 129S1 compared to B6 mice (28), while other studies reported either significant or insignificant weight gain in various strains of 129 mice compared to B6 on a HFD (29,30). The variation in 129 strain obesity resistance has led to several studies to determine the genetic or intestinal microbiota contributions in 129S1/B6 intercrossed animals (31,32). Results suggest genetic differences in 129S1 mice in metabolic and tissue responses to HFD. The current study aims to explore metabolic differences in response to excess DHT in NOD and 129S1 mice in comparison to those reported in B6 mice.

In B6 mice, 90-day DHT treatment causes ovarian dysfunction including estrous cycle irregularity, altered hormone secretion, and ovarian morphology. While the total number of ovarian follicles did not differ, ovaries of DHT treated mice had an increased number of atretic follicles with a cyst-like appearance and a hyperplastic theca cell area (19). Similar phenotypes were reported in mice treated with the aromatase inhibitor letrozole; but not in DHEA treated mice (18). Many of these ovarian phenotypes can be attributed to the expression of the androgen receptor (AR) specifically in theca-cells (33), of mice with a mixed (B6/CD1/129Sv) genetic background.

Excess androgens can lead to increased adiposity in mice and humans, and adiposity contributes to PCOS phenotype severity in women (8,9). White adipose tissue (WAT) is involved in energy storage, glucose homeostasis, inflammatory functions, and the endocrine system (34). Conversely, brown adipose tissue (BAT) is more metabolically active and is involved in thermodynamic processes for internal temperature regulation (35–37). Increased BAT is found to decrease obesity and increase weight loss as opposed to WAT, although recent studies have shown that browning of WAT (also called beige/brite fat) accompanied by altered gene expression has increased metabolic activity (37–39). Our current study examines the

4

1 metabolic and ovarian consequences of 90-day DHT treatment in prepubertal NOD and 129S1

2 mice to provide a novel way to examine genetic susceptibilities to PCOS.

3 **Materials & Methods**

4 **Animals:** All animal procedures were conducted in accordance with the National Institute of

5 Environmental Health Sciences Institutional Animal Care and Use Committee approval (Protocol

6 # 01-30). Animals were housed on a 12:12h light-dark cycle and fed NIH-31 chow and water ad

7 libitum. At PND19 or 20, female 129S1 (n=24) and NOD mice (n=32) were subcutaneously

8 implanted with placebo or DHT 90-day slow release pellets (2.5 mg) (Innovative Research of

9 America, Sarasota, FL). After implantation of pellets, animals were monitored daily for entrance

10 into puberty by vaginal opening. Animal weights were measured weekly. Estrous cycle was

11 monitored in females approximately 30 days after pellet implantation by performing vaginal

12 smears daily for 12 consecutive days. Cells were immediately fixed on glass slides with

13 cytology spray and stained with H&E following standard protocols. A single investigator staged

14 estrous cycle smears as previously described (40). At the duration of the study (90 days after

15 pellet insertion) anogenital distance (AGD) was measured using digital calipers, mice were

16 euthanized via CO_2 and tissues were collected as described below.

17 **Densitometry:** Densitometry was performed on day 83 after pellets were implanted. Mice were

18 anesthetized with isoflurane and imaged using a Piximus x-ray densitometer (GE Healthcare,

19 Piscataway, NJ, USA). Analysis outputs provided fat content and bone mineral density

20 measurements for each animal.

21 **Ovarian Morphology & Follicle Counting**: One ovary from each animal was immediately

22 weighed, fixed in 10% formalin. paraffin embedded following standard procedures and serial

23 sectioned (8 microns). Every 4th section was stained with H&E and follicles were classified and

24 counted based on size for a total of 10 slides per ovary. Follicles were classified similar to

25 Emmen et al.(41), small preantral follicles included an oocyte surrounded by 1 or 2 layers of

26 granulosa cells and large preantral follicles had an oocyte with 3-5 layers of granulosa cells.

Follicles that had an oocyte and more than 5 layers of granulosa cells and possibly some fluid were classified as small antral and large antral follicles had an oocyte with a single large fluid filled antrum (approximately 30% or more of the follicle). A follicle was only counted if an oocyte was present in the section. Follicles that appeared unhealthy (broken oocyte) and/or degenerate (fluid covering oocyte or improperly arranged or absent granulosa cells) were classed into a group without further classification (size unknown). The corpus lutea (CL) were also counted in each section. Investigators were blind to the treatment groups for each strain and data shown is the average ratings of two independent investigators.

Intraperitoneal Glucose Tolerance Test (IPGTT): Eighty-five days after pellet insertion, mice were fasted overnight for approximately 14 hours. Fasting glucose levels were measured using tail vein blood and a glucometer (Nova Biomedical). After initial (fasting) measurement, mice received intraperitoneal injections of 2g/kg glucose and tail vein blood was used to determine blood glucose levels at 20, 40, 60, 120 and 180 minutes after injection.

Adipose Tissue: Interscapular brown adipose and inguinal white adipose tissues were collected and snap frozen for gene expression analysis or fixed in 10% formalin and embedded in paraffin wax following established protocols. BAT and WAT were sectioned (8 microns) and stained using a standard H&E staining protocol for a total of 4 mice in each treatment group. Imaging of the BAT and WAT was done using an EVOSXL microscope, where 20x brightfield images were obtained and then analyzed (WAT only) using the WRI Adipocytes tool plug in ImageJ. For each section, researchers were blind to the treatment and manually outlined and counted 50 cells in two sections per animal to determine cell area.

Gene Expression: Interscapular BAT, inguinal WAT, and one ovary was collected and snap frozen at -80ºC. Tissues were pulverized and RNA was isolated using 1 mL (ovary) or 5 mL (adipose) of TRIzol® (Invitrogen, Carlsbad, CA) following manufacturer's instructions. RNA concentration was determined by spectrophotometry and cDNA was reverse transcribed using SuperScript (Invitrogen, Carlsbad, CA). cDNA was diluted and quantitative real-time PCR was

1 performed using SYBR Green (Invitrogen, Carlsbad, CA) with primer sequences available upon

2 request. Data are shown as a ratio of gene/*Rpl7* as described previously (42).

3 **Statistical Analysis:** Statistical analysis of body weight changes across 90 days was compared

4 using a mixed model ANOVA followed by Tukey's HSD test. In addition, to determine changes

5 in gene expression and final body weights, t-tests were used to compare treatment groups to

6 control in 129S1 and NOD mice using GraphPad Prism (GraphPad Software, La Jolla, CA).

7 Analysis of cell area for adipocytes was done using t-test comparisons of the average cell area

8 size in μm between control and DHT groups using the t.test()function in the R statistics

9 program.

10 **Results**

11 **Reproductive & Ovarian Phenotypes**

12 Female mice were treated with placebo or DHT for 90-days via a continuous release pellet

13 beginning at PND19. DHT significantly reduced the age of vaginal opening in both NOD (4.75

14 days early, p<0.001) and 129S1 mice (5.5 days early, p<0.001) compared to placebo treated

15 animals, which had vaginal opening at 31 days (NOD) or 29.5 days (129S1) (Fig. 1A-B). At the

16 end of the study, anogenital distance (AGD) increased by approximately 1.1 mm (p<0.001) in

17 DHT treated NOD and 129S1 mice (Figure 1C-D). Wet ovarian weight was significantly

18 decreased by DHT treatment in NOD mice (p<0.01), however, DHT did not significantly alter

19 ovarian weight in 129S1 mice (p=0.07) (Fig. 1E-F). These data demonstrate that DHT pellets in

20 both NOD and 129S1 mice altered AGDs similar to that observed in B6 mice following a similar

21 treatment protocol (Fig. S1(43)). To examine cyclicity in these animals, estrus cycles were

22 monitored for 12 days. While neither NOD nor 129S1 placebo mice had a normal 4-5 day cycle,

23 DHT altered the cycle pattern and significantly reduced the percentage of time in estrus for both

24 strains of mice. Cumulatively, NOD mice were in metaestrous and diestrous a higher

25 percentage of time and spent less time in proestrous suggesting that DHT induced an abnormal

26 estrous cycle although some did appear to ovulate after approximately 30 days of excess DHT.

1   129S1 mice did not show significant differences in other phases of the estrus cycle (Fig. S2

2   (43)), although more leukocytes were present in all phases of the estrous cycle in both placebo

3   and DHT treated 129S1 mice (data not shown).

4   Ovarian follicles were staged and counted to examine ovarian function. Previous reports found

5   that DHT reduces the presence of corpora lutea (CL) in B6 mice (18,19) (Fig. S3 (43)).

6   Interestingly, NOD and 129S1 mice had different ovarian phenotypes in the presence of excess

7   DHT (Fig. 2). NOD mice showed a trend to reduction in small preantral follicles (placebo 172±32

8   n=4; DHT 105±9 n=5, p=0.058), but a significant decrease in the number of large preantral

9   follicles (placebo 56.6±6.5 n=4; DHT 38±3.6 n=5, p<0.05). There was a drastic reduction in the

10   number of CLs compared to placebo treated NOD mice (placebo 4.0±1.4 n=4; DHT 0.2±0.2

11   n=5, p<0.01) (Fig. 2A-B). 129S1 mice had an insignificant increase in the number of small

12   preantral follicles in DHT group (placebo 86±13.8 n=4; DHT 138.5±22.9 n=5, p=0.08) and a

13   significant decrease in the number of small antral follicles (placebo 29.8±0.89 n=4; DHT.

14   24.1±1.3, p<0.01). While the 129S1 mice with DHT showed a trend towards more large antral

15   follicles in the ovary (placebo 0.9±0.2 n=4; DHT 2±0.4 n=5, p=0.053) this was not significant.

16   129S1 mice showed a significant decrease in the number of CLs present after DHT treatment

17   (placebo 8.6±2.9 n=4; DHT 1.3±0.8 n=5, p<0.05) (Fig. 2C-D). There was no difference observed

18   in the numbers of unhealthy or degenerative follicles or in the number of zona pellucida residues

19   in either NOD or 129S1 ovaries.

20   NOD and 129S1 mice had different ovarian morphology and DHT treatment exaggerated some

21   of these differences. Ovaries from placebo treated NOD mice showed the presence of several

22   CLs (Fig. 3A) although many of the ovarian follicles had unorganized granulosa cells making

23   assessment of the follicle stage difficult. Treatment of NOD mice with DHT led to decreased

24   follicles present in the ovary, and there were no clear CLs (Figure 3C). Regions of the ovary

25   appeared to look like possible CL and could be as some mice did go through estrus (Fig. S2

26   (43)), but they were not clearly defined as observed in the placebo treated NOD mice (Fig. 3A-

8

D). Ovaries of placebo treated 129S1 mice had follicles of many different sizes including the

presence of CLs. Their follicles had organized granulosa cells and well-formed thecal cell layers

(Fig. 3E-F). 129S1 ovaries in the presence of DHT show a thin layer of theca cells and

detachment of the theca cells from the GCs (Fig. 3G-H), although no large cystic follicles were

observed as reported in B6 mice (18,19).

To further study changes in ovarian function, expression of several steroidogenic

enzymes were examined including steroidogenic acute regulatory protein (*Star)*, P450 side

chain cleavage enzyme *(Cyp11a1)*, cytochrome P450c17a1 (*Cyp17*), and aromatase (*Cyp19)* in

NOD (Figure 4A) and 129S1 (Fig. 4B) ovaries. In NOD mice, DHT reduced the expression of

Star (4.0 fold, p<0.01) while expression was not altered in 129S1 mice. Expression of *Cyp11a1*

was reduced in both NOD (3.4 fold, p<0.01) and 129S1 (4.2 fold, p<0.01) mice. Expression of

Cyp17 was increased by DHT in NOD mice (6.9 fold, p<.0001) and unchanged in 129S mice.

Expression of *Cyp19* was not different in NOD mice, *Cyp19* expression was increased by DHT

in 129S1 mice (2.6 fold, p<0.05). Expression of several other steroidogenic genes including *3

beta-Hydroxysteroid dehydrogenase* and *17-beta hydroxysteroid dehydrogenase* was not

different in either strain (data not shown). DHT treatment did not alter the expression of the

androgen receptor (*Ar)* in either NOD or 129S1 ovaries. The expression of granulosa cell

specific Forkhead box L2 (*Foxl2*) was not different in NOD ovaries, while 129S1 ovaries had

reduced expression of *Foxl2* in the presence of DHT (1.3 fold, p<0.05) compared to placebo.

Expression of the luteinizing hormone/choriogonadotropin receptor (*Lhcgr*) was not different in

NOD ovaries, while its expression was increased in 129S1 ovaries (3.5 fold, p<0.01). Ovarian

expression of tissue inhibitor of metalloproteinases-1 (*Timp1*) was reduced in NOD ovaries (3.4

fold, p<0.05) while expression was not altered in 129S1 ovaries (Fig. 4).

Body Weight and Adipose Tissues Changes in Response to DHT

Animals were weighed weekly starting at 1 week after pellet implantation. Separate mixed

ANOVAs for the factors of treatment (DHT, placebo) and time (1-13 weeks) revealed main

9

1   effects of treatment and time on body weight as well as treatment x time interactions for both

2   NOD, $F_{(12, 360)}=17.7$, $p<0.0001$, $\eta^2=0.37$, and 129S1 mice, $F_{(12, 264)}=4.2$, $p<0.0001$,

3     $\eta^2=0.16$. Follow-up post-hoc comparisons of the DHT x time interactions revealed that, for NOD

4   mice, both the placebo and DHT conditions had significant increases in body weight over weeks

5   (i.e., placebo: 1<2; 4<5; 6<7; 8<9 weeks, ps<0.05; DHT: 1<2, 2<3; 4<5; 8<9 weeks, ps<0.001)

6   and the placebo and DHT conditions were significantly different from each other on all (ps<0.05)

7   but week 1. For 129S1 mice, both the placebo and DHT conditions had significant increases in

8   body weight over weeks (i.e, placebo: 1<2; 2<3; 8<9 weeks, ps<0.05; DHT: 1<2; 2<3; 4<5

9   weeks, ps<0.05) and the placebo and DHT conditions were significantly different from each

10   other each week of the study (p<0.05) (Fig. 5). Because of the differences in 129S1 mice

11   already present at week 1, we examined the final body weight of each animal and found that

12   DHT increased body weight in NOD mice (placebo 22.2±1.1 n=16; DHT 25.6±1.3 n=16,

13   p<0.0001) and 129S1 mice (placebo 21.2±1.2 n=12; DHT 23.1±1.2 n=16, p<0.001). The body

14   weight was not recorded at time of pellet insertion, therefore we also examined final change in

15   body weight from week 1 to week 13 and found DHT increased body weight in NOD (p<0.001)

16   and 129S1 mice (p<0.05). Animals were subjected to densitometry measurements which

17   showed no difference in total percent fat in either strain, while both NOD (2.0 g increase,

18   p<0.05) and 129S1 (1.4 g increase, p<0.001) mice showed an increase in the amount of lean

19   tissue in the DHT treated group. There were no differences in bone mineral density (Table 1)

20   between the treatment groups.

21   To examine glucose responsiveness, an IPGTT was performed at day 85 of treatment in each

22   strain of mice. While fasting blood glucose levels were not altered by DHT in either strain (NOD:

23   placebo 68.9 mg/dL vs DHT 73.2 mg/dL; 129S1: placebo 94.0 mg/dL vs DHT 88.8 mg/dL),

24   response to exogenous glucose was different. NOD mice had improved glucose tolerance when

25   treated with DHT compared to placebo treated animals. NOD mice naturally develop diabetes

26   (25,44,45) as demonstrated by the large increase in blood glucose levels and increased

1 clearance time within 180 minutes in the NOD placebo (Total AUC 23,371 ± 4,432, n=11) mice

2 compared to the 129S1 placebo (Total AUC 11,375 ± 1,878, n=12) treated animals (p<0.05).

3 Interestingly, NOD mice treated with DHT showed improved glucose tolerance as evidenced by

4 reduced maximum blood glucose concentrations (placebo 382.1 ± 62.20, n=11; DHT 241.5 ±

5 10.06, n=12, p<0.05) and reduced area under the curve from 0 to 180 minutes (placebo 23,371

6 ± 4,432, n=11; DHT 12,634 ± 772.6, n=12, p<0.05) (Fig. 6A-B). This finding is contradictory to

7 data in B6 mice where excess DHT leads to decreased glucose sensitivity (18,19) (Fig. S4

8 (43)).

9 The large difference in glucose response between the NOD placebo and DHT groups led us to

10 examine the hypothesis that excess testosterone alters glucose response in these mice by

11 performing an IPGTT with males that have higher endogenous testosterone levels. Age

12 matched NOD males were subjected to a IPGGT and have no significant difference in maximum

13 blood glucose concentrations compared to females in either group when analyzed by one-way

14 ANOVA (males 291±16.2, n=10). Male mice also had no significant difference in area under the

15 curve from 0 to 180 minutes (males 16,836 ± 1,511, n=10) compared to NOD female mice in

16 either treatment group (Fig. 6A-B). 129S1 mice did not show any differences in glucose

17 sensitivity when treated with DHT (Fig. 6 C-D).

18 Androgens have been shown to affect both the WAT and BAT in B6 mice (18,19); therefore we

19 examined WAT and BAT morphology and adipocyte size in the NOD and 129S1 mice.

20 Morphological changes were observed in both NOD and 129S1 mice treated with DHT

21 compared with placebo treated animals (Fig. 7A&C). In the BAT, both NOD and 129S1 mice

22 have increased oil red O staining in the DHT treated females compared to the placebo treated

23 group (Fig. S5 (43)). The size of the brown adipocytes was not measured due to limitations in

24 the WRI Adipocytes tool in ImageJ. NOD mice have a significant decrease in WAT cell size

25 (1,380.65 ± 36.31 SEM, p<0.05, n=350) while DHT increases WAT cell size in 129S1 mice

1 (12,241.96 ± 375.87 SEM, p<0.01, n=500) (Fig. 7B&D). Similar increases in WAT cell size have

2 been reported in B6 mice (18,19).

3 To further examine the adipose differences in the mouse strains, we examined gene expression

4 in WAT and BAT. RNA was isolated from WAT and BAT and the expression of genes important

5 for glucose tolerance including adiponectin (*Adipoq*) and the glucose transporter type 4 (*Glut4,*

6 officially *Slc2a4*) were measured. DHT increased expression of *Adipoq* in WAT of NOD mice

7 (2.1 fold, p<0.05) while there was no change in BAT or in 129S1 adipose tissue. Similarly, DHT

8 increased *Glut4* expression in the WAT of both NOD (2.6 fold, p<0.05) and 129S1 (1.4 fold,

9 p<0.001) mice. No significant differences were observed in the BAT of either strain, although

10 the NOD mice showed large variation in *Glut4* expression after DHT treatment (Fig. 8). Genes

11 involved in thermogenesis including the cell death-inducing DNA fragmentation factor, alpha

12 subunit-like effector (*Cidea*) and PR domain containing 16 (*Prdm16*) were also measured. The

13 WAT of NOD mice had increased expression of *Cidea* (4.3 fold, p<0.01), while the BAT showed

14 no significant change. *Cidea* expression was also unchanged in both adipose tissues in 129S1

15 mice. DHT exposure increased the expression of *Prdm16* in the WAT of both NOD (2.3 fold,

16 p<0.05) and 129S1 (3.7 fold, p<0.01) mice, however gene expression was not changed in BAT

17 of mice from either strain (Fig. 8). Expression of uncoupling protein 1 (*Ucp1*) was measured,

18 however no significant changes were observed potentially due to large variation within the

19 samples (data not shown). Genes involved in lipid storage including peroxisome proliferator-

20 activated receptor gamma (*Pparg*) and sterol regulatory element-binding protein (*Srebp*) *1a*, *1c*

21 and *2* were measured in BAT and WAT. Expression of *Pparg* was not altered in NOD adipose

22 tissue (slight increase in WAT by DHT; 1.4 fold, p=0.07), but had decreased expression in

23 129S1 WAT (7.1 fold, p<0.001). Expression of *Srebp1a* was increased in NOD WAT (1.9 fold,

24 p<0.01) and unchanged in BAT and 129S1 adipose tissues. The *Srebp1c* isoform significantly

25 increases in WAT (1.37 fold, p<0.05) and expression in BAT was decreased (1.7 fold, p=0.09)

1 the change was not significant in NOD mice (Fig. 8). Expression of *Srebp2* was not different in

2 any of the tissues examined (data not shown).

3 **Discussion**

4 It has been shown previously that 90-day DHT treatment induces both ovarian and metabolic

5 phenotypes in B6 mice (18,19). We hypothesized that NOD mice would have varied ovarian

6 responses due to development of T1D (46), while the ovarian response in 129S1 mice would be

7 similar to B6 mice. Herein, we show that DHT causes different ovarian and metabolic responses

8 in each strain of mice (summarized in Table 2).

9 Both NOD and 129S1 mice showed earlier puberty onset and long-term DHT treatment in NOD

10 mice had a significant reduction in the number of large preantral follicles and CLs present after

11 DHT treatment. NOD mice develop T1D as they age and it has been reported that as the

12 severity of T1D increases, the ovaries of NOD mice show increased numbers of atretic follicles

13 and atrophy in stromal cells (46). In our study, the number of degenerate or unhealthy follicles

14 was not different within the treatment groups, possibly due to the development of T1D. While B6

15 mice have been reported to have increased cystic-like follicles (18,19), these were not observed

16 in NOD or 129S1 ovaries.

17 The ovaries of NOD mice treated with DHT had reduced expression of *Star* and *Cyp11a1* and

18 *Timp1* as reported in B6 mice (33). *Timp1* is normally expressed in the growing follicles in the

19 ovary and suggested to have a role in follicle development and luteinization (47); global

20 knockout of *Timp1* leads to altered estrous cycles (48) and has been implicated in early

21 regression of the CL (47). In the ovaries of DHT treated NOD mice, there were several regions

22 that resembled a CL, however it was not a properly formed CL as observed in placebo treated

23 mice even though some animals did complete an estrus cycle. The reduction of *Timp1* may

24 contribute to the degenerate appearance of these CL-like structures in NOD mice as it relates to

25 PCOS.

1   Ovaries in DHT treated 129S1 mice had reduced numbers of CLs and follicles had theca cell

2   layers that were detached from the granulosa cells. 129S1 ovaries had a decrease in small

3   antral follicles that suggests reduced granulosa cell numbers, supported by reduced expression

4   of the granulosa cell specific gene *Foxl2*. An increase in the expression of *Lhcgr* was observed

5   in DHT treated 129S1 ovaries while expression of *Lhcgr* is reduced in B6 mice with PCOS (33)

6   and unchanged in NOD mice. Increased expression of LHCGR has been reported in theca cells

7   of women with PCOS (49) while another study found increased expression in granulosa cells

8   (50). 129S1 mice could provide insight into the differential expression of *LHCGR* in response to

9   PCOS.

10 The CYP19 gene has been implicated as a genetic modifier in women with PCOS, where

11 decreased allele length correlates with T levels (51) and associations of CYP19 gene variants

12 may be associated with assisted reproduction success (52). 129S1 mice had increased

13 expression of *Cyp19* while Ma et al. reported a reduction in *Cyp19* after DHT treatment in mice

14 with a mixed genetic background (B6/CD1/129Sv) (33). *CYP17* expression is increased in

15 women with PCOS (50) and contains a single nucleotide polymorphism that is correlated with

16 susceptibility (53). *CYP11A1*, another P450 enzyme that shows polymorphisms in certain

17 populations of women with PCOS associated with elevated testosterone levels (54), although

18 other studies contradict this (55,56). NOD and 129S1 mice have reduced expression of

19 *Cyp11a1*, and NOD mice have increased *Cyp17* expression. These varied results suggest

20 complex gene interactions in PCOS. Unfortunately we were unable to measure plasma steroid

21 hormone levels in these animals and examine how these gene expression changes correlate

22 with circulating hormones.

23 Glucose tolerance can be influenced by androgens and in B6 mice excess DHT leads to

24 glucose insensitivity in an IPGTT (18,19). However, NOD mice had the opposite effect, where

25 DHT improved glucose response and was similar to age matched NOD male mice. This effect

26 may be due to the differences reported in the development of insulitis in NOD males compared

to females (25). Our study found that excess DHT improves glucose tolerance in NOD female mice, although it does not alter fasting blood glucose levels. Steroid hormone treatment in neonatal NOD mice suggested hormonal imprinting might be the cause of differences in diabetic incidence (57). The intestinal microbiome in male and female NOD mice is significantly different and believed to contribute to the variation in incidence between sexes (58). Excess DHT in NOD females improves glucose tolerance, suggesting that postnatal testosterone may be the driving force for the sex differences observed (57). While the NOD mice showed improvement in the presence of excess DHT, glucose tolerance in 129S1 mice was not affected, possibly due to increased browning of WAT as reported in cold acclimated Sv129 mice (59).

Androgens have been implicated in regulating adiposity (60), and women with excess androgens have increased visceral adiposity (61). In WAT, NOD mice had decreased adipocyte size while 129S1 mice had increased adipocyte size consistent with B6 mice (18,19). Both NOD and 129S1 mice had increased body weights in response to DHT over the course of the study, however this doesn't correlate with changes in percent body fat or the differential adipose morphology observed between the two strains. Additionally, the body weight of NOD mice was not different at week 1 while the 129S1 mice showed treatment differences present at week 1 and maintained throughout the study. Unfortunately, the body weights of the animals was not recorded at time of pellet insertion making interpretation challenging, as it is unknown if the difference at week 1 in 129S1 mice is due to poor randomization or the DHT treatment. We compared the final body weights of the animals and found DHT increased body weight in both strains of mice compared to placebo treated animals. If the animals started out at different body weights prior to pellet insertion we would not see this from either of these analyses, therefore we also examined the overall change in body weight from week 1 to week 13 for each animal and found DHT increased changes in both NOD mice and 129S1. The discrepancy in adipocyte size and total percent body fat suggests that while some of the adipose stores may have changed, it is not significantly different in the whole body analysis. Further studies are

necessary to compare adipose morphology from different locations to understand the effect of androgens on total body adiposity in each strain and how this contributes to total body weight. NOD and 129S1 mice have similar BAT morphology following DHT treatment. To explore the differences observed in adipose tissue we looked at the expression of genes that regulate blood glucose levels including *Adipoq* and *Glut4*. In women with PCOS, enlarged adipocytes are associated with decreased adiponectin and insulin sensitivity (62), and testosterone has been shown to decrease adiponectin plasma concentrations (63). 129S1 mice, had no change in *Adipoq* expression levels, while adipocytes size did increase. Conversely, we found increased expression of *Adipoq* in WAT of NOD mice concurrent with decreased adipocyte size. The increase in *Adipoq* could contribute to reduced cell size in NOD mice,, however this may not correlate with secreted adiponectin levels that was not measured. The glucose transporter *Glut4* regulates blood glucose levels and is predominately found in adipose tissue and skeletal muscle (64). Women with PCOS have decreased *GLUT4*/GLUT4 expression in abdominal adipocytes (65,66), possibly due to increased expression of miRNA-93 (66). Both NOD and 129S1 mice show increased *Glut4* expression in adipocytes, that could contribute to the improved glucose tolerance in NOD mice and unchanged glucose tolerance in 129S1 mice after prolonged DHT exposure.

Adipose tissue plasticity contributes to altered thermogenesis in cold tolerance studies and suggested as a way to combat obesity (67) via thermogenic genes including *Cidea* and *Prdm16*. *Cidea* expression is increased in the WAT of NOD mice, while no significant changes were observed in 129S1 mice. *Cidea*/CIDEA is highly expressed in BAT and knockout mice have increased thermogenesis, metabolic activity, and energy expenditure. *Cidea* deficient mice have reduced adiposity, even on a HFD (68). Furthermore, increased *Cidea* expression in WAT generates metabolically healthy obese mice (69). The increased expression of *Cidea* after DHT in the NOD mice may be regulating the WAT and help improve their glucose tolerance even with increased body weight.

1   The fate of adipocytes relies on the expression of several genes including *Prdm16*, responsible

2   for controlling BAT identification. Knockout of *Prdm16* has been shown to reduce BAT

3   expression of *Cidea* and *Ucp1*, and overexpression of *Prdm16* increases expression (70). Both

4   NOD and 129S1 mice show increased *Prdm16* expression in the presence of DHT that may

5   lead to browning of the WAT, leading to improved glucose tolerance (NOD) or contributing to

6   the unaltered glucose metabolism in the 129S1 mice. Other studies have shown that 129S1

7   mice have increased browning of WAT compared to B6 mice (71), which is consistent with the

8   results observed where DHT increases expression of this gene in the WAT.

9   *Pparg* is involved in lipid synthesis and adipocyte differentiation though interactions with a

10 number of co-regulators (72). The expression of *Pparg* is significantly downregulated in 129S1

11 WAT as was seen in a rat model of PCOS (73), while NOD *Pparg* expression is unaltered. The

12 reduced expression of *Pparg* in 129S1 mice contradicts the increased expression of *Prdm16* as

13 these have been reported to form core transcriptional complex to regulate genes in adipocytes,

14 although *Ppara* has also been reported to regulate *Prdm16* (74). Lipid synthesis and secretion

15 could contribute to the altered adipocyte sizes, so we examined lipid secretion genes including

16 *Srebp1a* and *Srebp1c* and found expression is increased in NOD WAT, and unchanged in

17 129S1 WAT. *SREBP1* expression is increased in women with PCOS (75), and two

18 polymorphisms were identified that correlated with metabolic risk but not disease incidence (76).

19 An interaction between T1D and DHT in the NOD mice could explain the increased *Srepb1*

20 expression not observed in the 129S1 mice. The BAT had no significant changes in genes

21 expression, increased oil red O staining suggests increased lipid storage though not quantified.

22 Our study suggests changes in WAT may have more contributions to differential responses to

23 DHT and phenotypes observed.

24 The heterogeneous symptoms of PCOS in women have made genetic studies difficult. To date,

25 GWAS reviews (77–79) have identified several genes, although PCOS is believed to be a

26 complex genetic disease where the interaction of several genes and physiological responses

may contribute to the severity. Animal studies have provided novel insight into the mechanism of androgen excess, however, most of these studies are done in B6 mice which limits the ability to study genetic contributions to the phenotypes. Herein, we demonstrate that NOD and 129 mice have varied ovarian, metabolic, and adipose response to excess DHT and suggest that intercrosses between these strains could generate a novel PCOS animal model.

Acknowledgements

Data Availability

Original data generated and analyzed during this study are included in this published article or in the data repository listed in References.

References

1. Azziz R, Woods KS, Reyna R, Key TJ, Knochenhauer ES, Yildiz BO. The prevalence and features of the polycystic ovary syndrome in an unselected population. *J Clin Endocrinol Metab*. 2004;89(6):2745-2749. doi:10.1210/jc.2003-032046

2. Norman RJ, Dewailly D, Legro RS, Hickey TE. Polycystic ovary syndrome. *Lancet*. 2007;370(9588):685-697. doi:10.1016/S0140-6736(07)61345-2

3. Dumont A, Robin G, Catteau-Jonard S, Dewailly D. Role of Anti-Müllerian Hormone in pathophysiology, diagnosis and treatment of Polycystic Ovary Syndrome: A review. *Reprod Biol Endocrinol*. 2015;13(1). doi:10.1186/s12958-015-0134-9

4. Dumesic DA, Oberfield SE, Stener-Victorin E, Marshall JC, Laven JS, Legro RS. Scientific statement on the diagnostic criteria, epidemiology, pathophysiology, and molecular

genetics of polycystic ovary syndrome. *Endocr Rev.* 2015;36(5):487-525. doi:10.1210/er.2015-1018

5.   March WA, Moore VM, Willson KJ, Phillips DIW, Norman RJ, Davies MJ. The prevalence of polycystic ovary syndrome in a community sample assessed under contrasting diagnostic criteria. *Hum Reprod.* 2010;25(2):544-551. doi:10.1093/humrep/dep399

6.   Hampton T. NIH panel: Name change, new priorities advised for polycystic ovary syndrome. *JAMA - J Am Med Assoc.* 2013;309(9):863. doi:10.1001/jama.2013.1236

7.   Azziz R, Carmina E, Chen Z, et al. Polycystic ovary syndrome. *Nat Rev Dis Prim.* 2016;2. doi:10.1038/nrdp.2016.57

8.   Moran LJ, Norman RJ, Teede HJ. Metabolic risk in PCOS: Phenotype and adiposity impact. *Trends Endocrinol Metab.* 2015;26(3):136-143. doi:10.1016/j.tem.2014.12.003

9.   Barber TM, McCarthy MI, Wass JAH, Franks S. Obesity and polycystic ovary syndrome. *Clin Endocrinol (Oxf)*. 2006;65(2):137-145. doi:10.1111/j.1365-2265.2006.02587.x

10.   Walters KA, Allan CM, Handelsman DJ. Rodent Models for Human Polycystic Ovary Syndrome1. *Biol Reprod.* 2012;86(5). doi:10.1095/biolreprod.111.097808

11.   McNeilly AS, Colin Duncan W. Rodent models of polycystic ovary syndrome. *Mol Cell Endocrinol.* 2013;373(1-2):2-7. doi:10.1016/j.mce.2012.10.007

12.   H. Abbott D, E. Levine J, A. Dumesic D. Translational Insight Into Polycystic Ovary Syndrome (PCOS) From Female Monkeys with PCOS-like Traits.

13.   Padmanabhan V, Veiga-Lopez A. Sheep models of polycystic ovary syndrome phenotype. *Mol Cell Endocrinol.* 2013;373(1-2):8-20. doi:10.1016/j.mce.2012.10.005

14.   Dumesic DA, Abbott DH, Padmanabhan V. Polycystic ovary syndrome and its developmental origins. *Rev Endocr Metab Disord.* 2007;8(2):127-141. doi:10.1007/s11154-007-9046-0

15.   FRANKS S, MCCARTHY MI, HARDY K. Development of polycystic ovary syndrome: involvement of genetic and environmental factors. *Int J Androl.* 2006;29(1):278-285.

1   doi:10.1111/j.1365-2605.2005.00623.x

2   16.   Abbott DH, Nicol LE, Levine JE, Xu N, Goodarzi MO, Dumesic DA. Nonhuman primate

3   models of polycystic ovary syndrome. *Mol Cell Endocrinol*. 2013;373(1-2):21-28.

4   doi:10.1016/j.mce.2013.01.013

5   17.   Padmanabhan V, Veiga-Lopez A. Animal models of the polycystic ovary syndrome

6   phenotype. *Steroids*. 2013;78(8):734-740. doi:10.1016/j.steroids.2013.05.004

7   18.   Caldwell ASL, Middleton LJ, Jimenez M, et al. Characterization of Reproductive,

8   Metabolic, and Endocrine Features of Polycystic Ovary Syndrome in Female Hyperandrogenic

9   Mouse Models. *Endocrinology*. 2014;155(8):3146-3159. doi:10.1210/en.2014-1196

10   19.   van Houten ELAF, Kramer P, McLuskey A, Karels B, Themmen APN, Visser JA.

11   Reproductive and Metabolic Phenotype of a Mouse Model of PCOS. *Endocrinology*.

12   2012;153(6):2861-2869. doi:10.1210/en.2011-1754

13   20.   Azziz R. PCOS in 2015: New insights into the genetics of polycystic ovary syndrome.

14   *Nat Rev Endocrinol*. 2016;12(2):74. doi:10.1038/NRENDO.2015.230

15   21.   Threadgill DW, Miller DR, Churchill GA, de Villena FPM. The Collaborative Cross: A

16   Recombinant Inbred Mouse Population for the Systems Genetic Era. *ILAR J*. 2011;52(1):24-31.

17   doi:10.1093/ilar.52.1.24

18   22.   Welsh CE, Miller DR, Manly KF, et al. Status and access to the Collaborative Cross

19   population. *Mamm Genome*. 2012;23(9-10):706-712. doi:10.1007/s00335-012-9410-6

20   23.   Threadgill DW, Churchill GA. Ten years of the collaborative cross. *Genetics*.

21   2012;190(2):291-294. doi:10.1534/genetics.111.138032

22   24.   Anderson MS, Bluestone JA. THE NOD MOUSE: A Model of Immune Dysregulation.

23   *Annu Rev Immunol*. 2005;23(1):447-485. doi:10.1146/annurev.immunol.23.021704.115643

24   25.   BACH JF. Insulin-Dependent Diabetes Mellitus as an Autoimmune Disease. *Endocr*

25   *Rev*. 1994;15(4):516-542. doi:10.1210/edrv-15-4-516

26   26.   Crèvecoeur I, Gudmundsdottir V, Vig S, et al. Early differences in islets from prediabetic

NOD mice: combined microarray and proteomic analysis. *Diabetologia*. 2017;60(3):475-489.

doi:10.1007/s00125-016-4191-1

27.   Escobar-Morreale HF, Roldán-Martín MB. Type 1 diabetes and polycystic ovary

syndrome: Systematic review and meta-analysis. *Diabetes Care*. 2016;39(4):639-648.

doi:10.2337/dc15-2577

28.   Syn WK, Yang L, Chiang DJ, et al. Genetic differences in oxidative stress and

inflammatory responses to diet-induced obesity do not alter liver fibrosis in mice. *Liver Int*.

2009;29(8):1262-1272. doi:10.1111/j.1478-3231.2009.02036.x

29.   Fengler VHI, Macheiner T, Kessler SM, et al. Susceptibility of Different Mouse Wild Type

Strains to Develop Diet-Induced NAFLD/AFLD-Associated Liver Disease. Strnad P, ed. *PLoS*

One. 2016;11(5):e0155163. doi:10.1371/journal.pone.0155163

30.   Almind K, Kahn CR. Genetic determinants of energy expenditure and insulin resistance

in diet-induced obesity in mice. *Diabetes*. 2004;53(12):3274-3285.

doi:10.2337/diabetes.53.12.3274

31.   Su Z, Korstanje R, Tsaih SW, Paigen B. Candidate genes for obesity revealed from a

C57BL/6J x 129S1/SvImJ intercross. *Int J Obes*. 2008;32(7):1180-1189. doi:10.1038/ijo.2008.56

32.   Parks BW, Nam E, Org E, et al. Genetic control of obesity and gut microbiota

composition in response to high-fat, high-sucrose diet in mice. *Cell Metab*. 2013;17(1):141-152.

doi:10.1016/j.cmet.2012.12.007

33.   Ma Y, Andrisse S, Chen Y, et al. Androgen Receptor in the Ovary Theca Cells Plays a

Critical Role in Androgen-Induced Reproductive Dysfunction. *Endocrinology*. Published online

November 14, 2016:en.2016-1608. doi:10.1210/en.2016-1608

34.   Trayhurn P, Beattie JH. Physiological role of adipose tissue: white adipose tissue as an

endocrine and secretory organ. *Proc Nutr Soc*. 2001;60(3):329-339. doi:10.1079/pns200194

35.   Tseng YH, Cypess AM, Kahn CR. Cellular bioenergetics as a target for obesity therapy.

Nat Rev Drug Discov. 2010;9(6):465-481. doi:10.1038/nrd3138

1   36.   Cypess AM, Kahn CR. Brown fat as a therapy for obesity and diabetes. *Curr Opin*

2   *Endocrinol Diabetes Obes.* 2010;17(2):143-149. doi:10.1097/MED.0b013e328337a81f

3   37.   Fenzl A, Kiefer FW. Brown adipose tissue and thermogenesis. *Horm Mol Biol Clin*

4   *Investig.* 2014;19(1):25-37. doi:10.1515/hmbci-2014-0022

5   38.   Lee YH, Mottillo EP, Granneman JG. Adipose tissue plasticity from WAT to BAT and in

6   between. *Biochim Biophys Acta - Mol Basis Dis.* 2014;1842(3):358-369.

7   doi:10.1016/j.bbadis.2013.05.011

8   39.   Bartelt A, Heeren J. Adipose tissue browning and metabolic health. *Nat Rev Endocrinol.*

9   2014;10(1):24-36. doi:10.1038/nrendo.2013.204

10   40.   Jayes FL, Burns KA, Rodriguez KF, Kissling GE, Korach KS. The Naturally Occurring

11   Luteinizing Hormone Surge Is Diminished in Mice Lacking Estrogen Receptor Beta in the

12   Ovary1. *Biol Reprod.* 2014;90(2). doi:10.1095/biolreprod.113.113316

13   41.   Emmen JMA, Couse JF, Elmore SA, Yates MM, Kissling GE, Korach KS. In Vitro Growth

14   and Ovulation of Follicles from Ovaries of Estrogen Receptor (ER)α and ERβ Null Mice Indicate

15   a Role for ERβ in Follicular Maturation. *Endocrinology.* 2005;146(6):2817-2826.

16   doi:10.1210/EN.2004-1108

17   42.   Winuthayanon W, Piyachaturawat P, Suksamram A, et al. Diarylheptanoid

18   phytoestrogens isolated from the medicinal plant curcuma comosa: Biologic actions in vitro and

19   in vivo indicate estrogen receptor-dependent mechanisms. *Environ Health Perspect.*

20   2009;117(7):1155-1161. doi:10.1289/ehp.0900613

21   43.   Binder AK, Peecher DL, Qvigstad AJ, et al. Data From: Differential Strain-Dependent

22   Ovarian and Metabolic Responses in a Mouse Model of PCOS. *Figshare.* Date deposisted 24

23   November 2022 doi:10.6084/m9.figshare.21618894

24   44.   Pearson JA, Wong FS, Wen L. The importance of the Non Obese Diabetic (NOD)

25   mouse model in autoimmune diabetes. *J Autoimmun.* 2016;66:76-88.

26   doi:10.1016/j.jaut.2015.08.019

1   45.   Kikutani H, Makino S. The murine autoimmune diabetes model: NOD and related

2   strains. *Adv Immunol*. 1992;51:285-322. doi:10.1016/s0065-2776(08)60490-3

3   46.   Tatewaki R, Otani H, Tanaka O, Kitada JA. A morphological study on the reproductive

4   organs as a possible cause of developmental abnormalities in diabetic NOD mice. *Histol*

5   *Histopathol*. 1989;4(3):343-358.

6   47.   Goldman S. MMPS and TIMPS in ovarian physiology and pathophysiology Assisted

7   reproduction techniques View project towards safe and efficient cervical dilatation View project.

8   *Artic Front Biosci*. Published online 2004. doi:10.2741/1409

9   48.   Nothnick WB. Disruption of the Tissue Inhibitor of Metalloproteinase-1 Gene Results in

10 Altered Reproductive Cyclicity and Uterine Morphology in Reproductive-Age Female Mice1. *Biol*

11 *Reprod*. 2000;63(3):905-912. doi:10.1095/biolreprod63.3.905

12 49.   Comim F V., Teerds K, Hardy K, Franks S. Increased protein expression of LHCG

13 receptor and 17 -hydroxylase/17-20-lyase in human polycystic ovaries. *Hum Reprod*.

14 2013;28(11):3086-3092. doi:10.1093/humrep/det352

15 50.   Kanamarlapudi V, Gordon UD, López Bernal A. Luteinizing hormone/chorionic

16 gonadotrophin receptor overexpressed in granulosa cells from polycystic ovary syndrome

17 ovaries is functionally active. *Reprod Biomed Online*. 2016;32(6):635-641.

18 doi:10.1016/j.rbmo.2016.03.003

19 51.   Xita N, Lazaros L, Georgiou I, Tsatsoulis A. CYP19 gene: a genetic modifier of

20 polycystic ovary syndrome phenotype. *Fertil Steril*. 2010;94(1):250-254.

21 doi:10.1016/j.fertnstert.2009.01.147

22 52.   Lazaros L, Xita N, Hatzi E, et al. CYP19 gene variants affect the assisted reproduction

23 outcome of women with polycystic ovary syndrome. *Gynecol Endocrinol*. 2013;29(5):478-482.

24 doi:10.3109/09513590.2013.774359

25 53.   Liu X, Xu M, Qian M, Yang L. CYP17 T/C (rs74357) gene polymorphism contributes to

26 polycystic ovary syndrome susceptibility: evidence from a meta-analysis. *Endocr Connect*.

2021;10(12):R305-R316. doi:10.1530/EC-21-0327

54.	Pusalkar M, Meherji P, Gokral J, Chinnaraj S, Maitra A. CYP11A1 and CYP17 promoter polymorphisms associate with hyperandrogenemia in polycystic ovary syndrome. *Fertil Steril*. 2009;92(2):653-659. doi:10.1016/j.fertnstert.2008.07.016

55.	Daneshmand S, Weitsman SR, Navab A, Jakimiuk AJ, Magoffin DA. Overexpression of theca-cell messenger RNA in polycystic ovary syndrome does not correlate with polymorphisms in the cholesterol side-chain cleavage and 17α-hydroxylase/C17-20 lyase promoters. *Fertil Steril*. 2002;77(2):274-280. doi:10.1016/S0015-0282(01)02999-5

56.	Gaasenbeek M, Powell BL, Sovio U, et al. Large-Scale Analysis of the Relationship between CYP11A Promoter Variation, Polycystic Ovarian Syndrome, and Serum Testosterone. *J Clin Endocrinol Metab*. 2004;89(5):2408-2413. doi:10.1210/JC.2003-031640

57.	Hawkins T, Gala RR, Dunbar JC. The Effect of Neonatal Sex Hormone Manipulation on the Incidence of Diabetes in Nonobese Diabetic Mice. *Exp Biol Med*. 1993;202(2):201-205. doi:10.3181/00379727-202-43527

58.	Markle JGM, Frank DN, Mortin-Toth S, et al. Sex differences in the gut microbiome drive hormone-dependent regulation of autoimmunity. *Science (80-)*. 2013;339(6123):1084-1088. doi:10.1126/science.1233521

59.	Murano I, Barbatelli G, Giordano A, Cinti S. Noradrenergic parenchymal nerve fiber branching after cold acclimatisation correlates with brown adipocyte density in mouse adipose organ. *J Anat*. 2009;214(1):171-178. doi:10.1111/j.1469-7580.2008.01001.x

60.	Nohara K, Laque A, Allard C, Münzberg H, Mauvais-Jarvis F. Central mechanisms of adiposity in adult female mice with androgen excess. *Obesity*. 2014;22(6):1477-1484. doi:10.1002/oby.20719

61.	Evans DJ, Barth JH, Burke CW. Body fat topography in women with androgen excess. *Int J Obes*. 1988;12(2):157-162. Accessed January 16, 2020. http://www.ncbi.nlm.nih.gov/pubmed/3384560

24

62.   Mannerås-Holm L, Leonhardt H, Kullberg J, et al. Adipose Tissue Has Aberrant

Morphology and Function in PCOS: Enlarged Adipocytes and Low Serum Adiponectin, But Not

Circulating Sex Steroids, Are Strongly Associated with Insulin Resistance. *J Clin Endocrinol*

Metab. 2011;96(2):E304-E311. doi:10.1210/jc.2010-1290

63.   Nishizawa H, Shimomura L, Kishida K, et al. Androgens decrease plasma adiponectin,

an insulin-sensitizing adipocyte-derived protein. *Diabetes*. 2002;51(9):2734-2741.

doi:10.2337/diabetes.51.9.2734

64.   Huang S, Czech MP. The GLUT4 Glucose Transporter. *Cell Metab*. 2007;5(4):237-252.

doi:10.1016/j.cmet.2007.03.006

65.   Rosenbaum D, Haber RS, Dunaif A. Insulin resistance in polycystic ovary syndrome:

Decreased expression of GLUT-4 glucose transporters in adipocytes. *Am J Physiol - Endocrinol*

Metab. 1993;264(2 27-2). doi:10.1152/ajpendo.1993.264.2.e197

66.   Chen YH, Heneidi S, Lee JM, et al. Mirna-93 inhibits glut4 and is overexpressed in

adipose tissue of polycystic ovary syndrome patients and women with insulin resistance.

Diabetes. 2013;62(7):2278-2286. doi:10.2337/db12-0963

67.   Poher AL, Altirriba J, Veyrat-Durebex C, Rohner-Jeanrenaud F. Brown adipose tissue

activity as a target for the treatment of obesity/insulin resistance. *Front Physiol*. 2015;6(JAN).

doi:10.3389/fphys.2015.00004

68.   Zhou Z, Toh SY, Chen Z, et al. Cidea-deficient mice have lean phenotype and are

resistant to obesity. *Nat Genet*. 2003;35(1):49-56. doi:10.1038/ng1225

69.   Abreu-Vieira G, Fischer AW, Mattsson C, et al. Cidea improves the metabolic profile

through expansion of adipose tissue. *Nat Commun*. 2015;6. doi:10.1038/ncomms8433

70.   Harms MJ, Ishibashi J, Wang W, et al. Prdm16 is required for the maintenance of brown

adipocyte identity and function in adult mice. *Cell Metab*. 2014;19(4):593-604.

doi:10.1016/j.cmet.2014.03.007

71.   Soccio RE, Li Z, Chen ER, et al. Targeting PPAR? in the epigenome rescues genetic

1 metabolic defects in mice. *J Clin Invest*. 2017;127(4):1451-1462. doi:10.1172/JCI91211

2 72.   Corrales P, Vidal-Puig A, Medina-Gómez G. PPARs and Metabolic Disorders Associated

3 with Challenged Adipose Tissue Plasticity. *Int J Mol Sci*. 2018;19(7).

4 doi:10.3390/IJMS19072124

5 73.   Wang YX, Zhu WJ, Xie BG. Expression of PPAR-γ in adipose tissue of rats with

6 polycystic ovary syndrome induced by DHEA. *Mol Med Rep*. 2014;9(3):889-893.

7 doi:10.3892/MMR.2014.1895/HTML

8 74.   Sun C, Mao S, Chen S, Zhang W, Liu C. PPARs-Orchestrated Metabolic Homeostasis in

9 the Adipose Tissue. *Int J Mol Sci 2021, Vol 22, Page 8974*. 2021;22(16):8974.

10 doi:10.3390/IJMS22168974

11 75.   Shafiee MN, Mongan N, Seedhouse C, et al. Sterol regulatory element binding protein-1

12 (SREBP1) gene expression is similarly increased in polycystic ovary syndrome and endometrial

13 cancer. *Acta Obstet Gynecol Scand*. 2017;96(5):556-562. doi:10.1111/AOGS.13106

14 76.   Knebel B, Janssen OE, Hahn S, et al. Genetic variations in SREBP-1 and LXRa are not

15 directly associated to PCOS but contribute to the physiological specifics of the syndrome. *Mol*

16 *Biol Rep*. 2012;39(6):6835-6842. doi:10.1007/S11033-012-1508-0

17 77.   Hiam D, Moreno-Asso A, Teede HJ, et al. The Genetics of Polycystic Ovary Syndrome:

18 An Overview of Candidate Gene Systematic Reviews and Genome-Wide Association Studies. *J*

19 *Clin Med*. 2019;8(10). doi:10.3390/jcm8101606

20 78.   McAllister JM, Legro RS, Modi BP, Strauss JF. Functional genomics of PCOS: From

21 GWAS to molecular mechanisms. *Trends Endocrinol Metab*. 2015;26(3):118-124.

22 doi:10.1016/j.tem.2014.12.004

23 79.   Welt CK. Genetics of Polycystic Ovary Syndrome: What is New? *Endocrinol Metab Clin*

24 *North Am*. 2021;50(1):71-82. doi:10.1016/J.ECL.2020.10.006

25

26

1 **Figure Legends**

2 **Figure 1: Effects of DHT on Puberty, AGD, and Ovarian Weight.** After implantation of pellets,

3 age at vaginal opening was used as a measure of puberty (A-B). Anogenital Distance (C-D) and

4 Ovarian Wet Weight (E-F) corrected for body weight were determined at the end of the study.

5 Data shown are average ± SEM for NOD (n=16) and 129S1 (n=12). **, $p<0.01$, ***, $p<0.001$.

6 **Figure 2: Ovarian Follicle Numbers in NOD and 129S1 mice.** NOD (A-B) and 129S1 (C-D)

7 ovaries were fixed, paraffin embedded, serial sectioned (8-microns), and stained with H&E.

8 Follicles were staged and counted based by two independent researchers through 10

9 sections/ovary. Black bars are placebo and grey bars are DHT. Data shown are the average

10 total follicle numbers ± SEM for a total of 4-5 animals per group. Data were analyzed via an

11 unpaired student t-test. *, $p<0.05$.

12 **Figure 3: Ovarian Histology.** Whole ovaries were formalin fixed, paraffin embedded, and

13 tissues were cut into 8-micron sections and stained with H&E for placebo (A-B, E-F) and DHT

14 (C-D, G-H) treatment groups in NOD (A-D) and 129S1 (E-H) mice. Representative sections are

15 shown at 10X and 20X magnification from different ovaries to demonstrate ovarian morphology

16 including CL (corpora lutea) and separation between theca and granulosa cells marked by white

17 arrows in 129S1 ovaries (G-H). Scale bars equal 400 μm (10X) or 200 μm (20X).

18 **Figure 4: DHT Mediated Alterations in Ovarian Gene Expression.** Whole ovarian RNA was

19 isolated and reverse transcribed into cDNA from NOD (A) and 129S1 (B) mice. Real-Time

20 qPCR was performed using primers specific for each gene and each treatment where black

21 bars are placebo and grey bars are DHT. Genes included steroidogenic genes *Star*, *Cyp11a1,*

22 *Cyp17* and *Cyp19* and ovarian genes *Ar*, *Foxl2*, *Lhcgr* and *Timp1*. Data shown is the average ±

23 SEM with a minimum of 5 animals per group. Data were analyzed via an unpaired student t-test.

24 *, $p<0.05$, **, $p<0.01$. ****, $p<0.0001$.

25 **Figure 5: Body weight in NOD and 129S1 mice.** Average body weights were measured each

26 week for NOD (A) and 129S1 (B) mice. Data shown are average ± SEM for NOD (n=16) and

27

1   129S1 (n=12). Data were analyzed using a mixed effects ANOVA which revealed treatment x

2   time interactions for both NOD and 129S1 mice ($p<0.0001$) followed by multiple comparisons by

3   Tukey's HSD. *, difference between treatment groups ($p<0.05$).

4   **Figure 6: Glucose Responsiveness in NOD and 129S1 mice.** At day 85 of the study, mice

5   were fasted overnight and subjected to an intraperitoneal glucose tolerance test. Fasting blood

6   glucose was measured using a glucometer for both NOD (A) and 129S1 (C) and then 2000

7   mg/kg body weight glucose was injected via an intraperitoneal injection. Blood glucose was

8   measured at 20, 40, 60, 120 and 180 minutes. Data shown is average ± SEM for NOD and

9   129S1 mice (n=12/group except for NOD placebo where n=11 and NOD male n=10). The area

10   under the curve from 0-180 minutes for NOD (B) and 129S1 (D) mice. Data shown is average ±

11   SEM and analyzed via one-way ANOVA for NOD mice and an unpaired student t-test for

12   129S1. *, $p<0.05$.

13   **Figure 7: Changes in Adipose Tissue Morphology.** Paraffin embedded tissues were cut into

14   8-micron sections and stained with H&E for placebo and DHT treatment groups in NOD (A) and

15   129S1 (C) mice. Brown and white adipose cell images are representative images from n=5 mice

16   examined in each treatment group. Scale bars equal 200 μm. Average white adipose cell area

17   was determined using ImageJ for NOD (B) and 129S1 (D) for control and DHT subjects. Data

18   shown is adipose cell average in n=5 per each group. Average of cell area for each treatment

19   group is compared using t-tests. *, $p<0.05$.

20   **Figure 8: Gene Expression Differences in NOD and 129S1 Adipose Tissue.** White Adipose

21   Tissue (WAT) and Brown Adipose Tissue (BAT) was isolated from animals, RNA was isolated

22   and reverse transcribed into cDNA. Real-Time qPCR was performed using primers specific for

23   each gene where black bars are placebo and grey bars are DHT. Genes studied include two

24   glucose responsive genes Adiponectin (*Adipoq*) (A&H), Gl*ut4* (officially *Slc2a*) (B&I) and two

25   genes implicated in thermogenesis including the cell death-inducing DNA fragmentation factor,

26   alpha subunit effector A (*Cidea)* (C&J) and the PR domain containing 16 (*Prdm16*) (D&K). Lipid

1 storage genes including peroxisome proliferator-activated receptor gamma (*Pparg*) (E&L) and

2 sterol regulatory element-binding protein (*Srebp*1a) (F&M) and (*Srebp*1c) (G&N). Data shown is

3 the average ± SEM with a minimum of 5 animals per group. Data were analyzed via an unpaired

4 student t-test for each adipose type and specific to each strain of mice. *, p<0.05, **, p<0.01.

5

6 **Table 1: Body Composition Changes in Response to DHT**

	NOD Mice		129 Mice	
	Placebo	**DHT**	**Placebo**	**DHT**
Total % Fat	12.41 ± 0.61 (n=16)	12.88 ± 0.55 (n=16)	15.56 ± 0.63 (n=12)	17.63 ± 1.09 (n=12)
Total Lean Tissue (g)	18.46 ± 0.23 (n=16)	20.58 ± 0.23 (n=16)*	15.24 ± 0.28 (n=12)	16.63 ± 0.15 (n=12)***
Bone Mineral Density (g/cm^2)	0.0544 ± 0.006 (n=16)	0.069 ± 0.016 (n=16)	0.128 ± 0.048 (n=12)	0.056 ± 0.0007 (n=12)

7 *, p<0.05; ***, p<0.001

8

9 **Table 2: Summary of Physiological Results in Response to DHT**

	NOD	**129S1**	**C57BL/6**
Vaginal Opening	4.75 days early*	5.5 days early*	ND
AGD	increased (1.1 mm)*	increased (1.1 mm)*	increased*
Ovarian Wet Weight	decreased*	NS	increased*
Time in Estrus / Estrus Cycle	decreased* / abnormal	decreased* / abnormal	ND
Ovarian Morphology	decreased preantral follicles & CLs*	decreased small antral follicles & CLs*	cystic follicles & reduced CLs *[18,19]
Overall Body Weight	increased*	increased*	increased*
IPGTT	improved sensitivity*	NS	decreased sensitivity*
White Adiopcyte Size	decreased*	increased*	increased*[18,19]

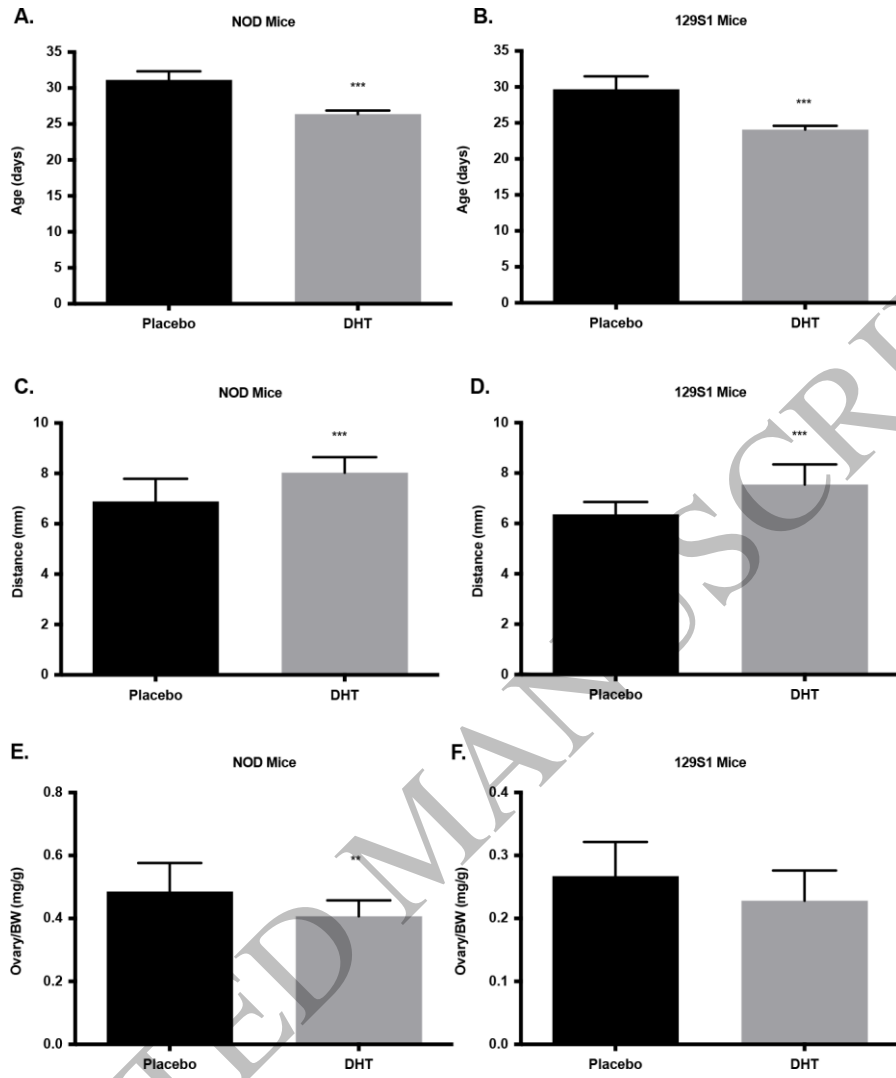10 *, p<0.05; NS, Not Significant; ND, Not Determined

11

Figure 1
118x140 mm (.14 x DPI)
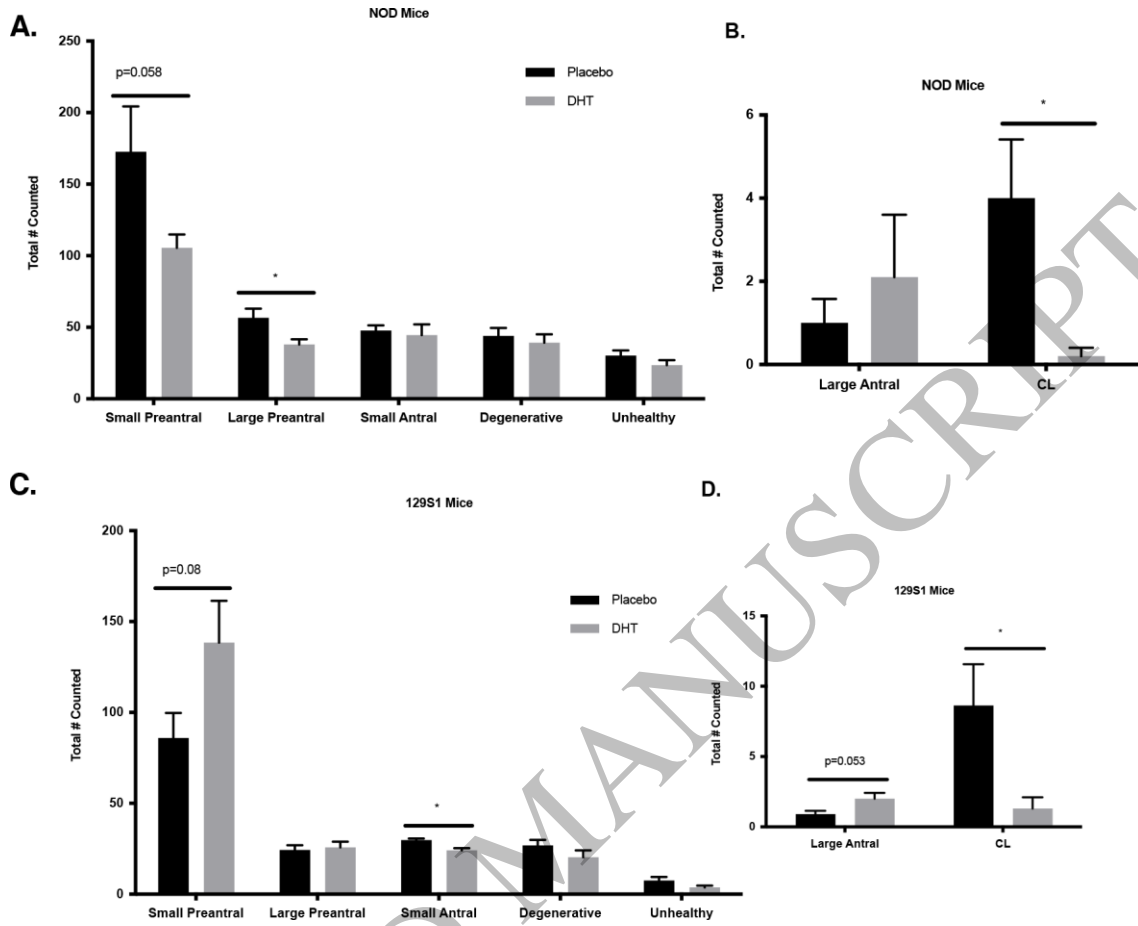
Figure 2
149x120 mm (.14 x DPI)

1

2
3

4

10X

20X

Placebo

A.

B.

CL

CL

DHT

C.

D.

129S1 Mice

10X

20X

Placebo

E.

F.

CL

DHT

G.

H.
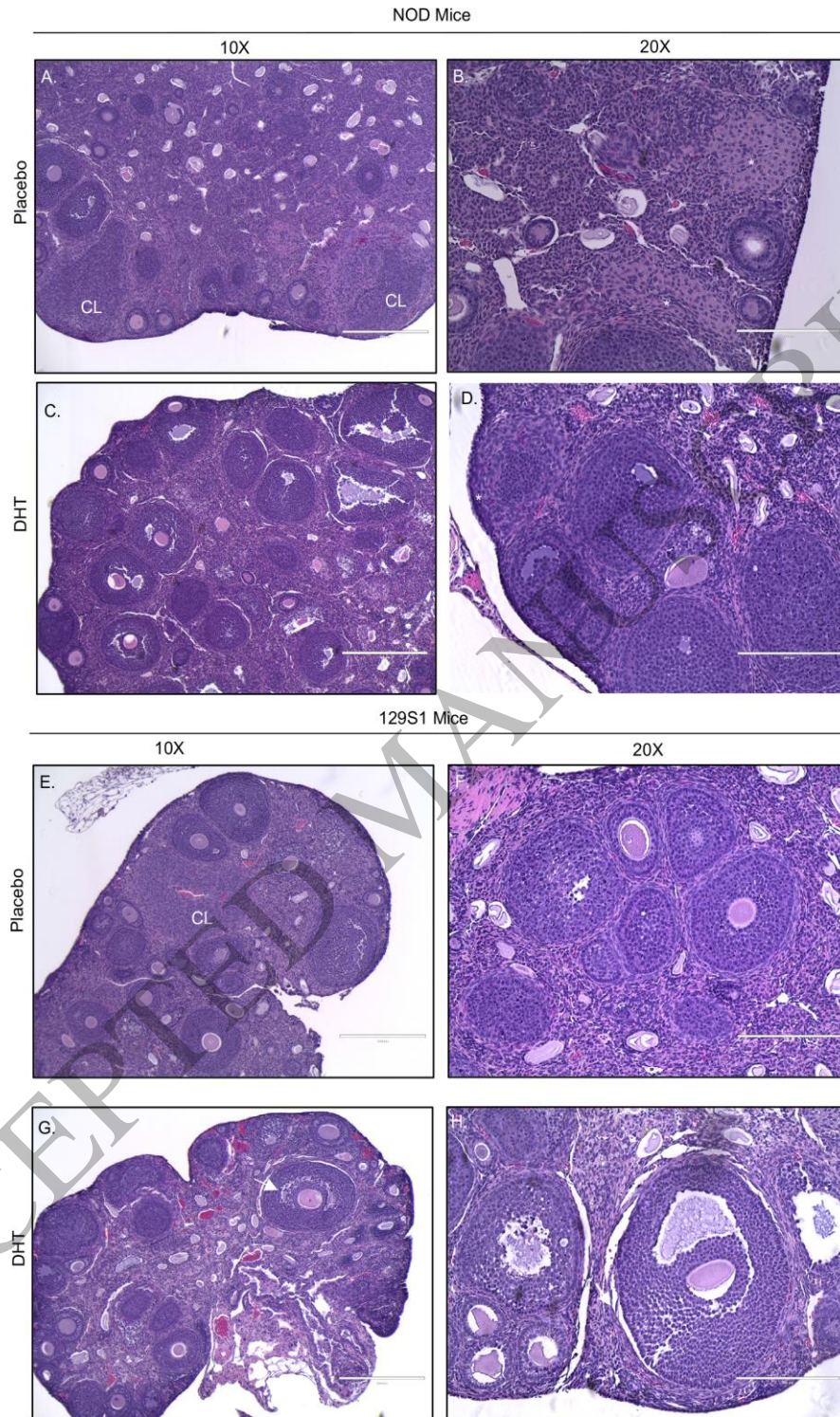
Figure 3
140x226 mm (.14 x DPI)
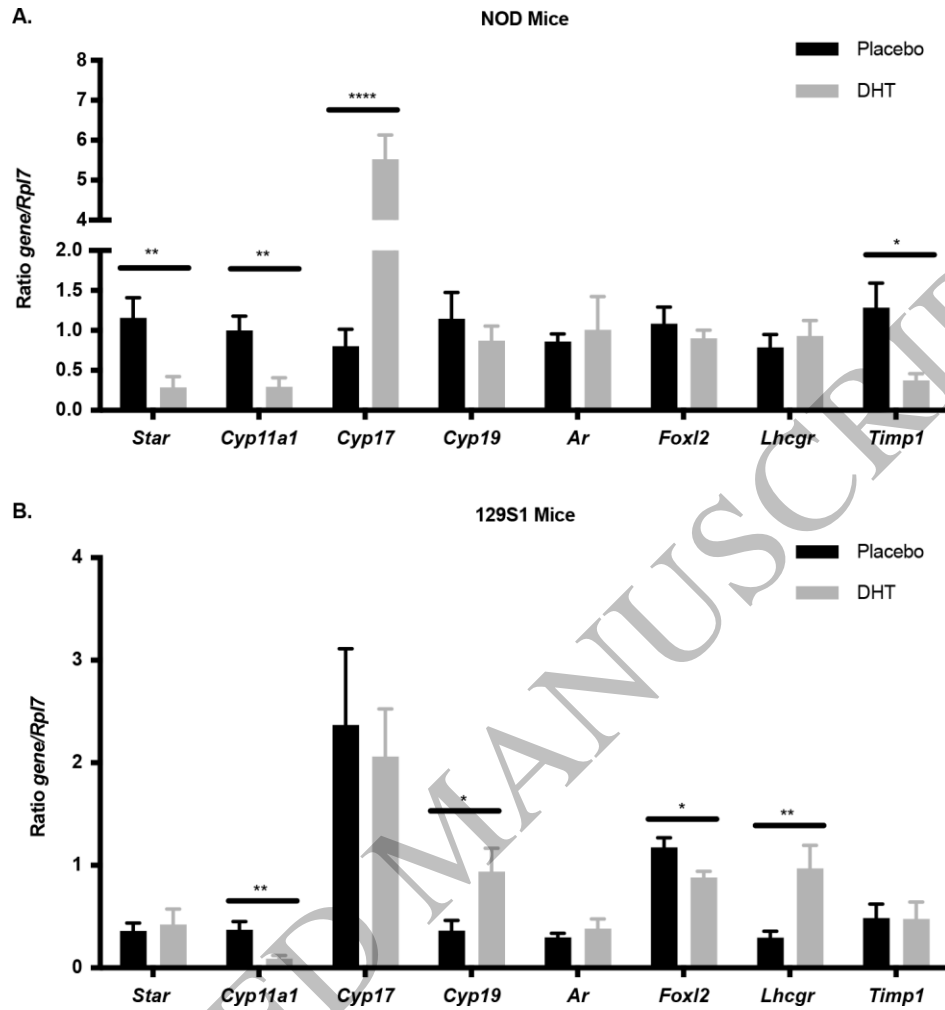
Figure 4
124x132 mm (.14 x DPI)

A.

NOD Mice

B.

129S1 Mice

1
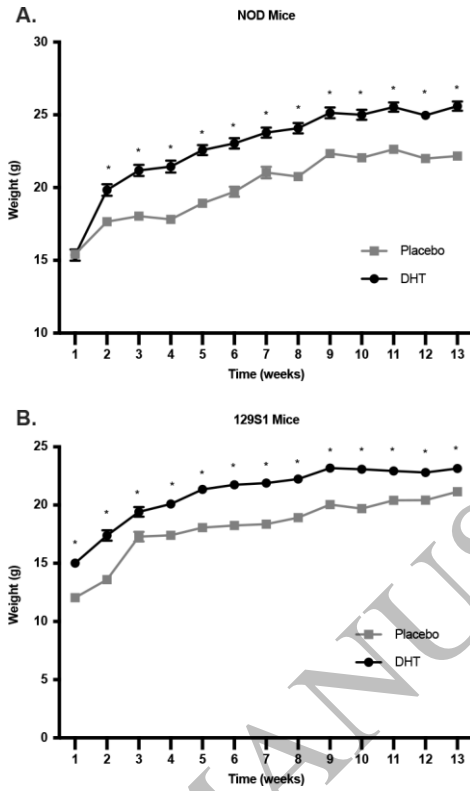
2   **Figure 5**

3   **62x103 mm (.14 x DPI)**
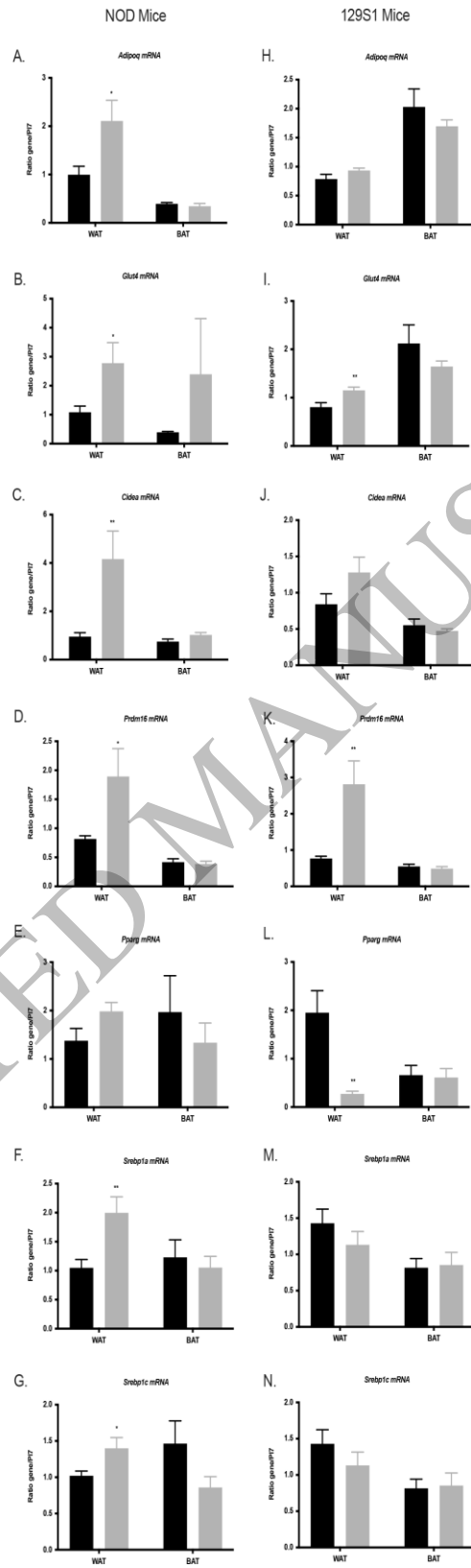
4
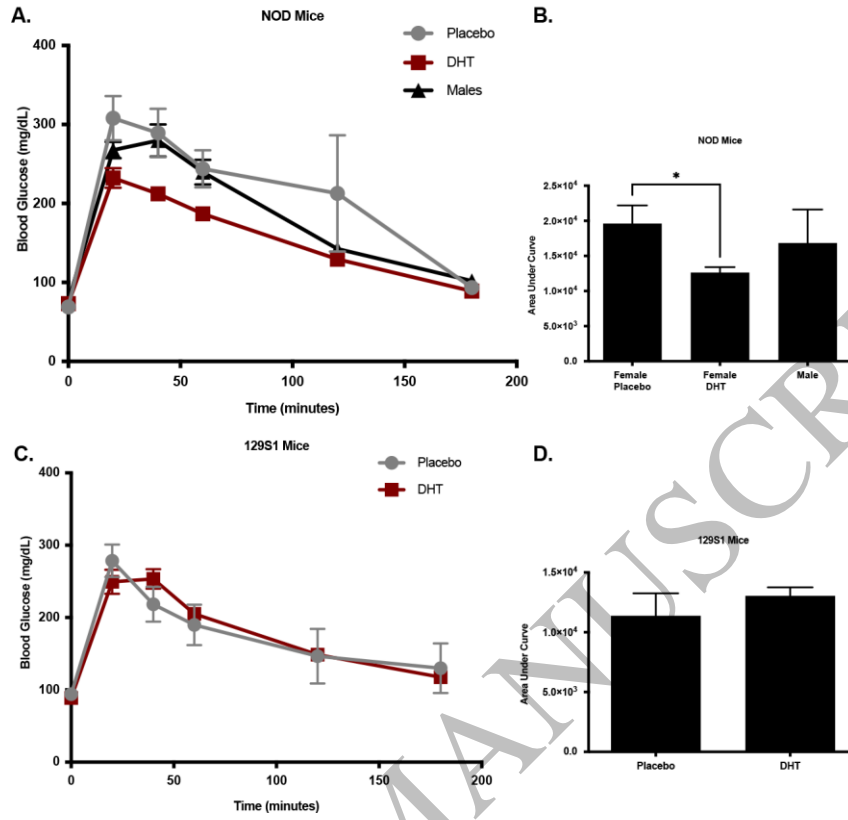
Figure 6
112x108 mm (.14 x DPI)
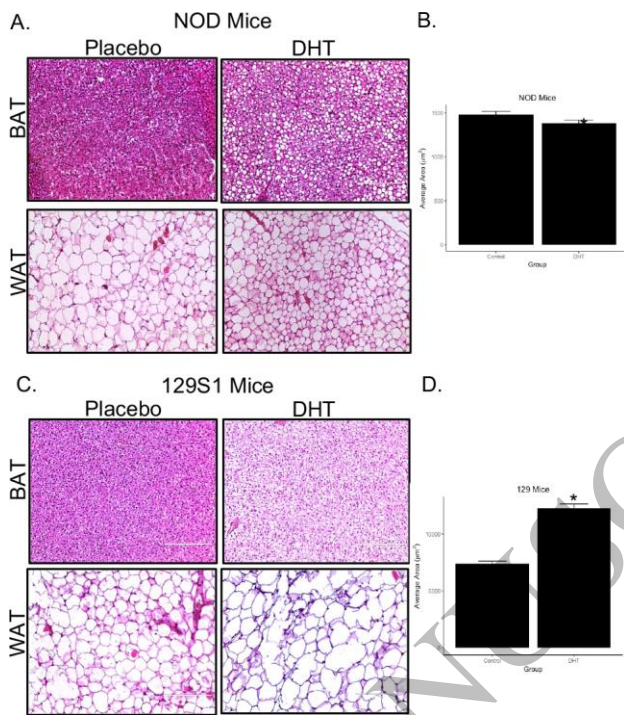
Figure 7
82x93 mm (.14 x DPI)

Figure 8
84x229 mm (.14 x DPI)